Bruton tyrosine kinase covalent inhibition shapes the immune microenvironment in chronic lymphocytic leukemia

Daniel Medina-Gil,[1,2] Laura Palomo,[1,2] Víctor Navarro,[3] Gonzalo Lázaro,[4] Beatriz Martín-Mur,[5] Cristina Hernández,[1,2] Oriol Castells,[1,2] Belén Sánchez,[1,2] Pau Marc Muñoz-Torres,[6] Carlota Pagès,[1,2] Gemma Pujadas,[1,2] Anna Esteve-Codina,[5] Alba Cabirta,[2,7] Christelle Ferrà,[8] Miguel Alcoceba,[9] Maria José Terol,[10] Rafael Andreu,[11] Mercè Martí,[4] Pau Abrisqueta,[2,7] Francesc Bosch[2,7] and Marta Crespo[1,2] on behalf of the Spanish Group of Chronic Lymphocytic Leukemia (GELLC)

[1]Experimental Hematology, Vall d'Hebron Institute of Oncology (VHIO), Vall d'Hebron Barcelona Hospital Campus, Barcelona; [2]Department of Medicine, Universitat Autònoma de Barcelona, Bellaterra; [3]Oncology Data Science (ODysSey) Group, Vall d'Hebron Institute of Oncology (VHIO), Vall d'Hebron Barcelona Hospital Campus, Barcelona; [4]Immunology Unit, Department of Cell Biology, Physiology and Immunology, Institut de Biotecnologia i Biomedicina (IBB), Universitat Autònoma de Barcelona, Bellaterra; [5]CNAG-CRG, Center for Genomic Regulation, Barcelona Institute of Science and Technology, Barcelona; [6]Bioinformatic Unit, Vall d'Hebron Institute of Oncology (VHIO), Vall d'Hebron Barcelona Hospital Campus, Barcelona; [7]Servei d'Hematologia, Vall d'Hebron Hospital Universitari, Experimental Hematology, Vall d'Hebron Institute of Oncology (VHIO), Vall d'Hebron Barcelona Hospital Campus, Barcelona; [8]Department of Hematology, Institut Català d'Oncologia - Hospital Germans Trias i Pujol, Josep Carreras Research Institute, Badalona; [9]Department of Hematology, Cancer Research Institute of Salamanca, University Hospital of Salamanca, Salamanca; [10]Department of Hematology, Hospital Clínico Universitario de Valencia, Valencia and [11]Department of Hematology, Hospital Universitario Politécnico "La Fe", Valencia, Spain

Correspondence: M. Crespo
macrespo@vhio.net

F. Bosch
fbosch@vhio.net

Received: September 17, 2024.
Accepted: February 28, 2025.
Early view: March 13, 2025.

https://doi.org/10.3324/haematol.2024.286663

Abstract

Continuous treatment with ibrutinib not only exerts tumor control but also enhances T-cell function in patients with chronic lymphocytic leukemia (CLL). We conducted longitudinal multi-omics analyses in samples from CLL patients receiving ibrutinib upfront to identify potential adaptive mechanisms to Bruton tyrosine kinase (BTK) inhibition during the first 12 months of continuous therapy. We found that ibrutinib induced a decrease in the expression of exhaustion markers and the proportion of regulatory T cells and T-follicular helper cells normalized to levels observed in healthy donors. Functionally, the expression of genes related to activation, proliferation, differentiation, and metabolism were downregulated in T cells; after *in vitro* stimulation, proliferation capacity was only slightly modified by ibrutinib treatment, while cytokine production was increased. In CLL cells, we observed a downregulation of immunosuppression, adhesion, and migration proteins. Adaptation at molecular level, characterized by an increase in cancer cell fraction of CLL cells with mutated driver genes, was observed in around half of the patients and was associated with retained migrative capacity towards CXCL12/CXCR4 axis. Interestingly, *BTK* C481S mutations were detected as early as after 6 months of treatment, particularly enriched in subsets of malignant cells retaining migrative capacity. These CLL cells with potential migrative capacity under ibrutinib also exhibited a distinct transcriptomic profile including upregulation of mTOR-AKT and MYC pathways. We identified the high expression of *TMBIM6* as a potential novel independent poor prognostic factor. Of note, BIA, a TMBIM6 antagonist, induced CLL cell apoptosis and synergized with ibrutinib. In summary, our comprehensive multi-omics analysis of CLL patients undergoing ibrutinib therapy has unveiled early immunomodulatory effects on T cells and adaptative mechanisms in CLL cells. These findings can contribute to the identification of resistance mechanisms and the discovery of novel therapeutic targets.

Introduction

Bruton tyrosine kinase (BTK) inhibition with ibrutinib is currently used in both treatment-naïve and relapsed/refractory CLL patients.[1,2] BTK inhibition in B cells mainly blocks B-cell receptor (BCR) signaling, which translates into diminished cell survival and proliferation. This inhibition also reduces homing capacity, leading to the release of CLL cells from secondary lymphoid organs and bone marrow (BM) into peripheral blood (PB), which deprives malignant cells of the supportive niche.[3-6]

CLL is characterized by a marked T-cell dysfunction, including a pseudo-exhausted phenotype, defective immune synapse formation, and accumulation of effector memory T cells and regulatory T cells (Tregs)[7,8] that aggravates from diagnosis to clinical progression.[9] Several reports indicate that ibrutinib improves T-cell function by reducing the pseudo-exhaustion, the number of Tregs, and by polarizing T-helper (Th) cells towards Th1.[10-12] The immunomodulatory effects of ibrutinib are often attributed to its off-target inhibition of ITK, primarily observed *in vitro*.[13,14] Similar effects have been reported in patients, though some inconsistencies exist across reports.[11,12,15]

Patients receiving continuous treatment with ibrutinib rarely achieve undetectable minimal residual disease (uMRD) and have cumulative risk of discontinuation due to adverse events or progression, which is often caused by selection of subclones carrying *BTK* mutations that impede covalent union of the drug to its target.[16] The elucidation of the adaptation mechanisms to BTK inhibition may help to overcome future resistances and to identify potential novel targets that can help improving the quality and depth of the clinical response.

The Spanish Group of CLL (GELLC) recently conducted the GELLC-7 trial, a multi-center phase II study aiming to determine whether consolidation with monoclonal antibody anti-CD20 ofatumumab improves the response in treatment-naïve CLL patients receiving ibrutinib. Thus, previously untreated patients received 12 cycles of ibrutinib monotherapy at 420 mg. Patients not attaining a complete remission (CR) after this induction continued with ibrutinib and received an additional consolidation with seven doses of ofatumumab, whereas those achieving a CR also continued ibrutinib until progression or exceeding toxicity.[17] Using PB samples from patients included in the trial, we longitudinally evaluated the changes within the immune compartment, as well as the phenotypic and molecular evolution of malignant CLL cells over the course of a 12-month period of ibrutinib treatment. This enabled us to assess the impact of ibrutinib on T-cell functionality and to identify adaptive mechanisms employed by CLL cells in response to BTK covalent inhibition. This unveiled novel potential targets that could inform the prospective design of new therapeutic consolidation strategies aiming to achieve deeper responses.

Methods

Patient samples

A total of 26 patients from the GELLC-7 clinical trial (*clinicaltrials gov. Identifier: NCT03280160*) with two or more samples of the longitudinal study were included. The median age of the study cohort was 65 years (range, 48-82 years). Of the patients, 21 of 26 (81%) were male, and 19 of 26 (73%) had unmutated *IGHV* (*Online Supplementary Table S1*). Additional peripheral blood mononuclear cells (PBMC) from seven treatment-naïve CLL patients were used for *in vitro* cell cultures. PBMC from ten age-matched healthy donors (HD) with a median age of 65 years (range, 64-69 years) were also analyzed as a reference control group. A written informed consent was obtained from all individuals in accordance with the declaration of Helsinki and the study was approved by the local clinical research ethics committee.

Flow cytometry

Cells were stained at $10x10^6$ cells/mL in a final volume of 100 μl of phosphate-buffered saline + bovine serum albumin (BSA) 0.5% + 0.1% sodium azide at room temperature for 15 minutes. Fluorochrome-conjugated antibody information is listed in *Online Supplementary Table S2* (see Extended methods in the *Online Supplementary Appendix*).

T-cell proliferation and cytokine production assays

PBMC from CLL patients were labeled with carboxylfluorescein succinimidyl ester (Thermo Fisher Scientific) (5 μM). Cells were stimulated with Dynabeads Human T-Activator CD3/CD28 (Gibco) in a ratio of 1:10 T cells for 3 days at $5x10^6$ cells/mL in 200 μL of complete IMDM GlutaMAX media (Gibco). Levels of soluble proteins related to immune response were measured with the LEGENDplex Human CD8/NK Panel (13-plex) (Biolegend). Proliferation and cytokine production levels of PBMC from six age-matched HD cultured at $1x10^6$ cells/mL were also measured as a reference control group (see Extended methods in the *Online Supplementary Appendix*).

For intracellular staining, 2 million PBMC from CLL patients and age-matched HD were stimulated with PMA (50 ng/mL) and ionomycin (1 μg/mL) (Biolegend) with Golgi inhibition with 5 μg/mL of brefeldin A (Biolegend) for 4 hours (h) at 37°C 5% CO2 in 1 mL of complete IMDM GlutaMAX media (Gibco). Extracellular staining included CD107a-APC and major T-cell subpopulations. Intracellular staining included granzyme B-FITC (Biolegend) (1:50) and IFNγ-PC7 (Thermo Fisher Scientific) (1:50) (see Extended methods in the *Online Supplementary Appendix*).

Chemokine determination

Chemokine determination in plasma was performed by using a custom ProcartaPlex Immunoassay kit of Luminex (Thermo Fisher Scientific). Duplicates and triplicates for each sample were included (see Extended methods in the *Online Supplementary Appendix*).

Migration assay

B cells were isolated by using EasySep Human B Cell Enrichment w/o CD43 Depletion kit (Stem cell) and 2x10^6 cells in 100 μL were added on the 24-well polystyrene inserts of 5.0 μm pore size (Corning). Cells were allowed to migrate towards CXCL12 (200 ng/mL) (Peprotech) in RPMI media + BSA 0.5% (Sigma-Aldrich) for 4 h in triplicates at 37°C (see Extended methods in the *Online Supplementary Appendix*).

Targeted DNA sequencing

DNA was sequenced with a custom next-generation sequencing (NGS) panel targeting codifying regions of 190 genes commonly mutated in hematological malignancies (*Online Supplementary Table S3*). Libraries were sequenced on a NovaSeq 6000 (Illumina) instrument, with a 2x150 bp paired-end standard protocol at a mean depth of coverage of 2,000x, to detect variants with a variant allele frequency (VAF) down to 1% (see Extended methods in the *Online Supplementary Appendix*).

RNA sequencing

Total RNA was isolated from purified T cells or migrating isolated B cells. For each sample, one paired-end library was prepared using the SMARTseq2 protocol18. Samples were run on NovaSeq 6000 (Illumina) with a read length of 2x50 bp paired-end (see Extended methods in the *Online Supplementary Appendix*).

Chronic lymphocytic leukemia cell cultures

For suspension cultures, PBMC were thawed and plated in 48-well plates at a concentration of 2x10^6 cells/mL in a total volume of 0.5 mL of AIM-V media supplemented with 2% human plasma and 50 μM β-mercaptoethanol. After 30 minutes of resting at 37°C, cells were treated with increasing concentration of BIA (Axon MedChem) for 48 h. Co-cultures of PBMC with BM stromal cells (BMSC) were performed as previously described.[19] Cells were treated with increasing concentration of BIA (Axon MedChem) and ibrutinib (MedChemExpress) for 24 h. Synergy scores were calculated by using Synergyfinder20 (see Extended methods in the *Online Supplementary Appendix*).

Statistical analysis

See Extended methods in the *Online Supplementary Appendix*.

Results

Upfront ibrutinib treatment alters the absolute numbers of immune cells in chronic lymphocytic leukemia patients

PBMC and plasma were longitudinally collected from whole blood obtained from 26 CLL patients included in the GELLC-7 trial. The samples were obtained at a minimum of two time points: before treatment (BT), and at 1 month, 3 months, 6 months, and 12 months following the initiation of ibrutinib treatment. To perform a longitudinal assessment of the concurrent evolution of immune and malignant cells throughout the treatment, multi-omics analyses were performed. These analyses encompassed flow cytometry, RNA sequencing (RNAseq), cytokine and chemokine determinations, proliferation assays, migration assays, and targeted DNA sequencing (targeted-DNAseq) (Figure 1).

Flow cytometric analysis showed the expected progressive decrease in CLL cell percentage during ibrutinib treatment, accompanied by an enrichment in T cells, natural killer (NK) cells and monocytes, as well as a peak in absolute lymphocyte count after 1 month, followed by normalization of blood counts (*Online Supplementary Figure S1A-E*). Furthermore, CD4$^+$ T cells were significantly enriched after 3 months of ibrutinib, leading to an inversion of the CD4/CD8 ratio (*Online Supplementary Figure S1F-H*). The composition of NK cells, including immature (CD56^{br}CD16$^-$) and highly cytotoxic NK cells (CD56^{dim}CD16$^+$), remained unaltered (*Online Supplementary Figure S2A*). Additionally, no changes were found in monocyte subpopulations, including classical (CD14^{++}CD16$^-$), intermediate (CD14^{++}CD16$^+$), and non-classical (CD14$^+$CD16^{++}) (*Online Supplementary Figure S2B*). These results indicate that ibrutinib initially releases CLL cells and other immune cells from lymph nodes (LN) or BM into the PB, with subsequent normalization of absolute numbers as the tumor regresses.

Ibrutinib reverts phenotypic features associated with T-cell dysfunction in chronic lymphocytic leukemia

T cells in CLL patients exhibit a dysfunctional phenotype resembling pseudo-exhaustion, characterized by conserved cytokine production and an inability to form effective immune synapses. These cells also show elevated expression of exhaustion markers, including PD-1, CD244 and CD160.[7-9] In our cohort, baseline analysis showed that the most abundant T-cell subsets were effector memory and effector memory-RA in CD8$^+$, and central memory and effector memory in CD4$^+$ T cells (*Online Supplementary Figure S3A-D*). The analysis of the distribution of T-cell differentiation subsets during ibrutinib treatment showed no variations after 12 months compared to BT. However, there was a significant decrease in the percentage of CD8$^+$ and CD4$^+$ T cells expressing PD-1 overtime, although levels remained higher than the ones observed in aged-matched HD, indicated by the dashed red line (Figure 2A; *Online Supplementary Figure S4A*). CD244 expression was higher than that observed in HD only for CD8$^+$ T cells and an initial reduction was observed in the first months in both CD8$^+$ and CD4$^+$ T cells that was not further maintained (Figure 2B; *Online Supplementary Figure S4B*). T cells also exhibited a reduction of the expression of other exhaustion-related proteins, CD39 and TIGIT, that reached values similar to

those observed in HD (Figure 2C, D; *Online Supplementary Figure S4C, D.*). CD160 expression was only found in CD8$^+$ T cells and decreased upon 12 months of ibrutinib, although expression levels were still over those observed in HD-derived CD8$^+$ T cells (Figure 2E; *Online Supplementary Figure S4E*). In our cohort, T cells were predominantly negative for TIM3 and LAG-3, similar to what was observed in HD (*data not shown*). Most of the exhaustion markers were co-expressed with PD-1, and this double-expressing populations also diminished after 12 months of ibrutinib monotherapy. Interestingly, although PD-1 expression remained higher in CLL, co-expression of PD-1 with CD39 and TIGIT decreased over time to values similar to HD (*Online Supplementary Figure S5A-G*). Overall, ibrutinib treatment lowers the expression of markers associated with pseudo-exhaustion in CLL.

Regarding CD4$^+$ Th cells, previous reports have indicated increased Tfh, Th1, Th2, and Th17 levels in PB of CLL patients compared to HD.[21-24] Additionally, Treg frequency is also higher in CLL.[23] In our series, we observed a reduction in the percentage of Tfh cells after 12 months of ibrutinib treatment (Figure 2F; *Online Supplementary Figure S6A*). The immunosuppressive Tregs were reduced already after 1 month of treatment and progressively decreased up to 12 months reaching levels similar to those observed in HD (*Online Supplementary Figures 2F* and *S6B*). The frequency of Th1 cells was lower after 12 months of ibrutinib treatment, while Th2 and Th17 subpopulations remained mainly unchanged (*Online Supplementary Figure S6C, D*). Thus, ibrutinib influenced CD4$^+$ Th cells by reducing Tfh, Tregs and Th1 subpopulations that are enriched and play a tumor-supportive role in CLL.[25,26]

Proliferation capacity of T cells from chronic lymphocytic leukemia patients after *ex vivo* stimulation is normalized by ibrutinib treatment, while cytokine release capacity increases

Next, we characterized genome-wide transcriptional changes in T cells upon ibrutinib treatment. To address this, we isolated CD3$^+$ cells from 11 paired samples at BT and after 6 months of treatment (median purity ~94%, assessed by flow cytometry; *Online Supplementary Figure S7*) and performed bulk RNAseq analysis. Over 200 genes were identified as differentially expressed (DEG), 54 of them upregulated and 151 downregulated. Unsupervised hierarchical clustering based on the DEG categorized the paired samples into two different clusters, corresponding with the ibrutinib treatment groups (Figure 3A; *Online Supplementary Table S5*). Overrepresentation pathway analysis (ORA) with downregulated genes revealed 110 significantly enriched Gene

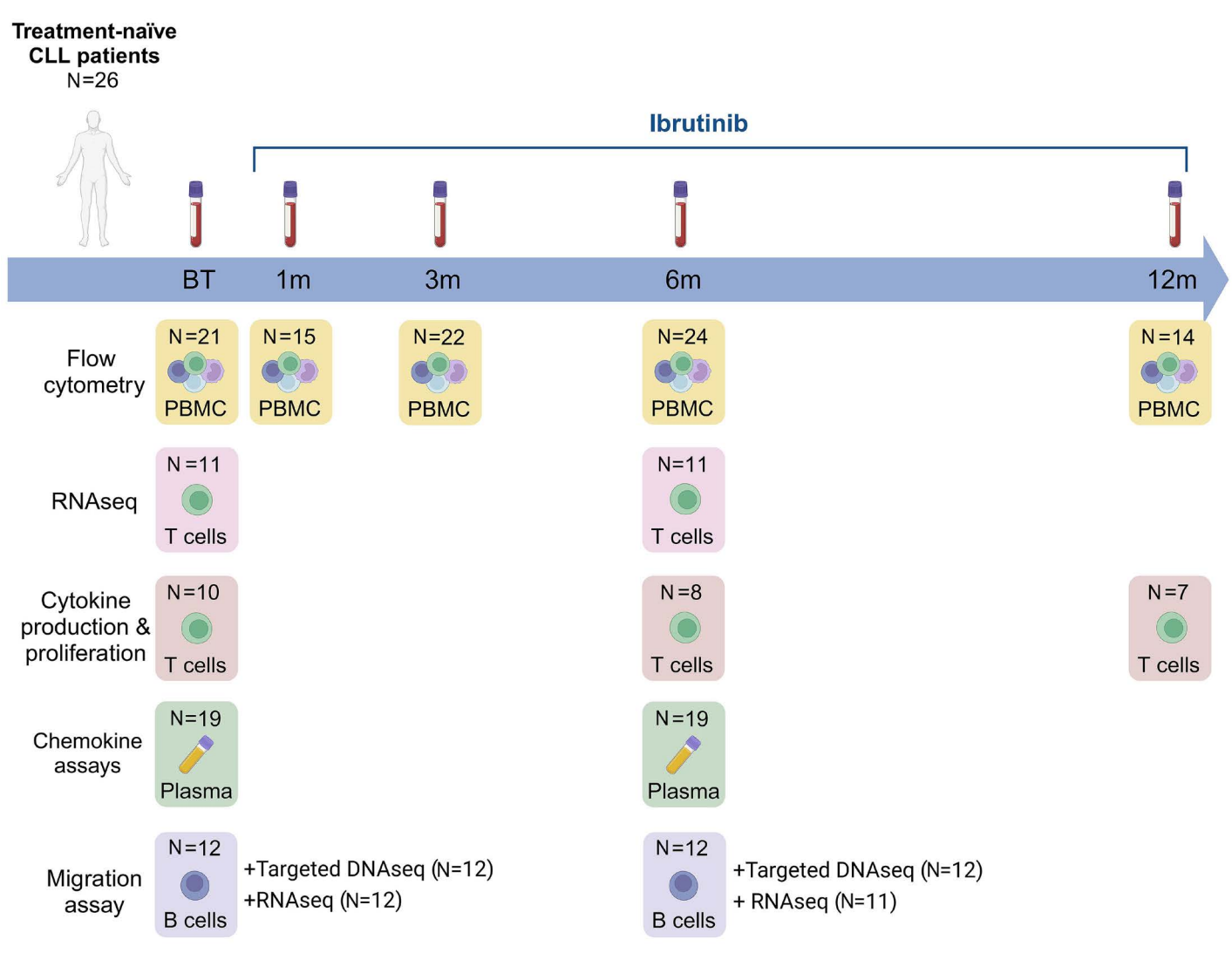

Figure 1. Schematic representation of the multi-omics analyses of GELLC-7 clinical trial samples. BT: before treatment; PBMC: peripheral blood mononuclear cells; 1-12m: 1-12 months after treatment; DNAseq: DNA sequencing; RNAseq: RNA sequencing. CLL: chronic lymphocytic leukemia.

Ontology biological processes (*Online Supplementary Table S6*). REVIGO clustering of these processes disclosed a predominant relation to immune response and regulation of cell activation[27] (*Online Supplementary Figure S8A*). Further ORA of downregulated genes against KEGG and Reactome databases revealed an enrichment of terms related to T-cell activation, such as Th differentiation, PD-1 signaling or phosphorylation of CD3 and TCR ζ chains (Figure 3B; *Online Supplementary Table S6*). Gene set enrichment analysis (GSEA) demonstrated negative regulation of activation (interferon γ response and allograft rejection), metabolism (e.g., glycolysis or reactive oxygen species pathway) and proliferation processes (E2F targets and G2M checkpoint) (Figure 3C; *Online Supplementary Table S7*). Collectively, these data show that ibrutinib not only reduces the expression of exhaustion markers and immunosuppressive cell subpopulations, but also downregulates pathways associated with T-cell activation, proliferation, differentiation, and metabolism which may indicate a restoration of a quiescent state more comparable to healthy conditions.

Deconvolution of T-cell subpopulations using RNAseq data was performed using the CIBERSORTx algorithm.[28] Data showed a significant increase in memory activated CD4$^+$ T cells and a marked decreased in Tfh cells upon ibrutinib treatment as observed in flow cytometry analyses (*Online Supplementary Figure S8B*; *Online Supplementary Table S4*). T cells from CLL patients show increased expression of exhaustion markers, defects in proliferation but maintain cytokine secretion capacity, therefore they are considered to be in a pseudo-exhausted state.[8] To evaluate the effect of ibrutinib on T-cell function in our cohort, we initially assessed the proliferation capacity upon unspecific T-cell receptor (TCR) stimulation using beads coated with anti-CD3/CD28. After 3 days of culture, a significant but modest decrease of proliferating CD4$^+$ T cells was observed, while CD8$^+$ T cells retained proliferation capacity upon 12 months of ibrutinib, both showing a tendency to approach levels similar to those observed in HD (Figure 3D). Next, to assess the cytotoxic potential of T cells after ibrutinib treatment, we analyzed the expression of CD107a, gran-

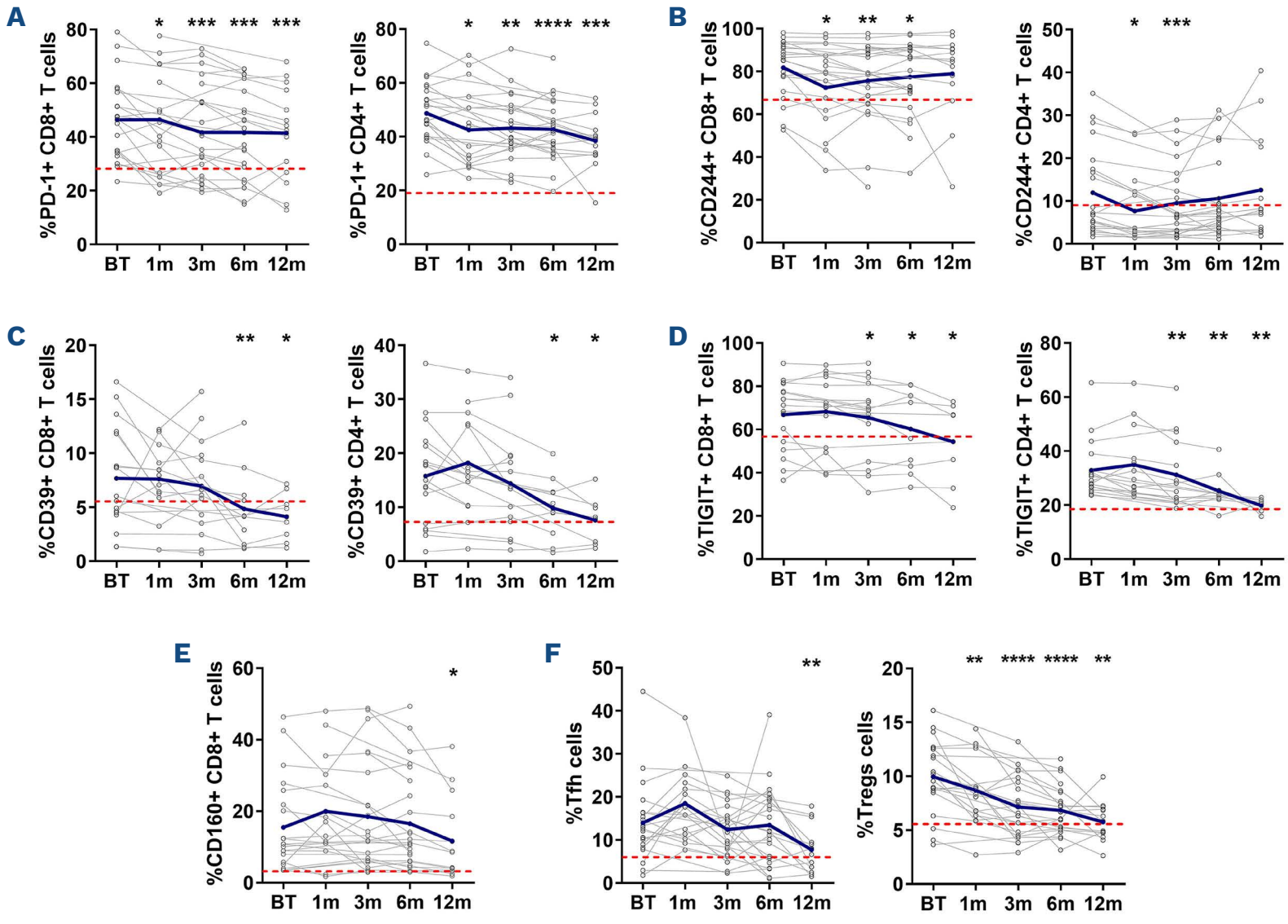

Figure 2. Immunophenotypic effect of ibrutinib on T cells. (A-D) Longitudinal analysis of the PD-1, CD244, CD39 and TIGIT expressions during ibrutinib treatment in CD8$^+$ and CD4$^+$ T cells. (E) Longitudinal analysis of the CD160 expression during ibrutinib treatment in CD8$^+$ T cells. (F) Longitudinal analysis of the percentage of T-follicular helper (Tfh) cells defined as CXCR5$^+$CD4$^+$ T cells and regulatory T cells (Tregs) defined as CD25$^+$CD127$^{lo/-}$ CD4$^+$ T cells. Flow cytometry analyses included before treatment (BT) N=21, 1 month after treatment (1m) N=15, 3m N=22, 6m N=24 and 12m N=14 samples. Wilcoxon matched paired signed rank test was performed to compare statistical differences between BT and the subsequent time points. Grey lines represent the dynamics of individual patients, while the blue line represents the mean values across all patients. Red dashed line represents the mean value of age-matched healthy donors (HD) (N=10). *P<0.05; **P<0.01; ***P<0.001; ****P<0.0001.

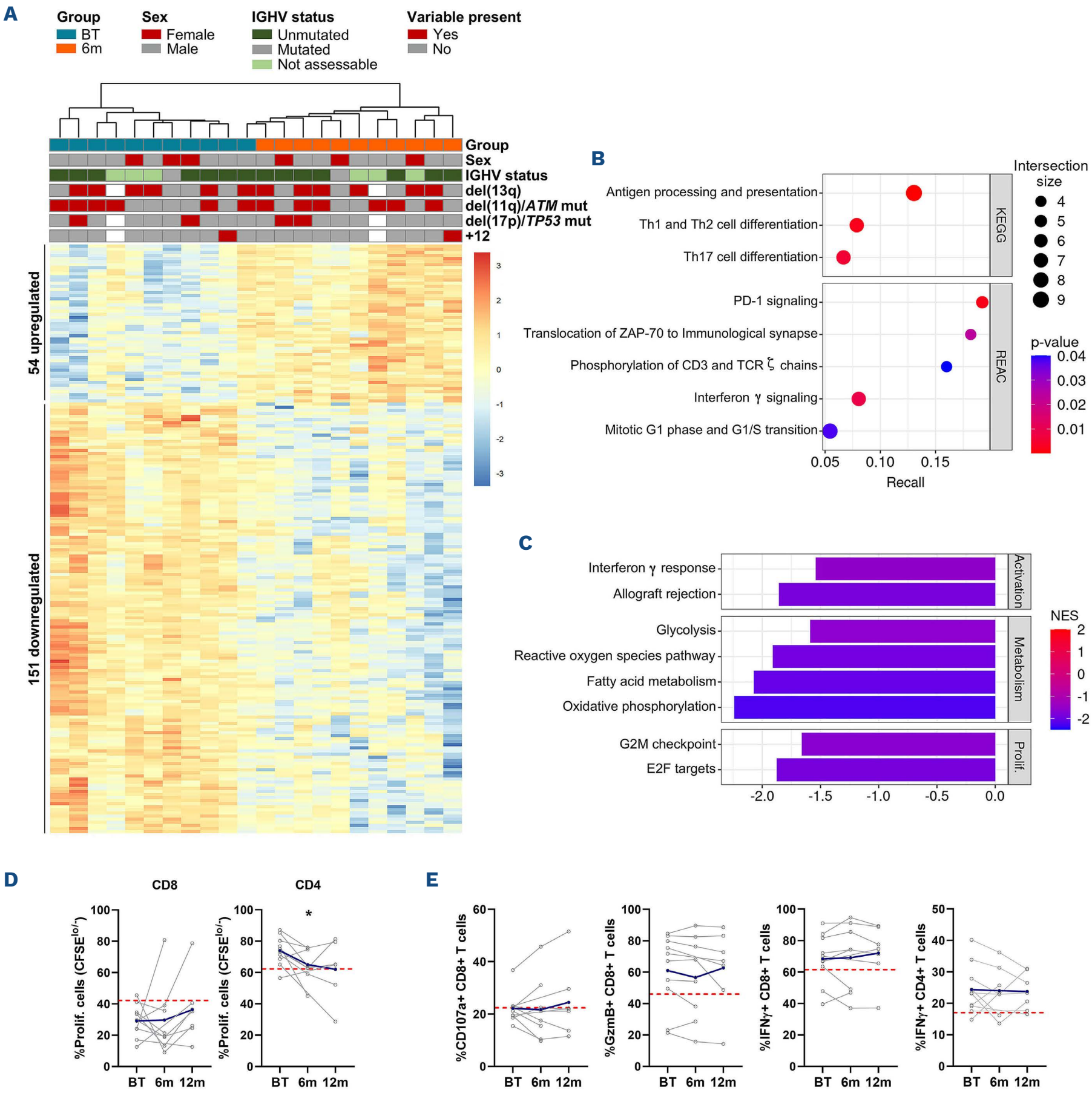

Figure 3. Transcriptomic and functional effect of ibrutinib on T cells. (A) Clustered heatmap of the differential expressed genes (DEG) (false discovery rate [FDR]<0.05) in T cells after 6 months of ibrutinib treatment compared to before treatment (BT). (B) Dot plot of a summary of the significantly enriched terms of Kyoto Encyclopedia of Genes and Genomes (KEGG) and Reactome gene set databases from the overrepresentation analysis with the downregulated DEG. Intersection size represents the number of DEG present in a specific gene set and recall represents the intersection size divided by the number of genes of the specific gene set. (C) Summary of the significantly enriched processes (FDR<0.05) from the gene set enrichment analysis (GSEA) against Hallmarks from MSigDB. (D) Effect of ibrutinib in the percentage of proliferating CD8$^+$ and CD4$^+$ T cells (CFSE$^{lo/-}$) after 3 days of unspecific T-cell receptor (TCR) stimulation with Dynabeads Human T-Activator CD3/CD28. (E) Effect of ibrutinib on the expression of CD107a and granzyme B (GzmB) in CD8$^+$ T cells and interferon γ (IFNγ) in CD8$^+$ and CD4$^+$ T cells upon 4 hours of PMA/Ionomycin stimuli. Wilcoxon matched paired signed rank test was performed to compare statistical differences between BT and the subsequent time points. Grey lines represent the dynamics of individual patients, while the blue line represents the mean values across all patients. Red dashed line represents the mean value of age-matched healthy donors (HD) (N=6). *P<0.05; **P<0.01; ***P<0.001; ****P<0.0001. 6m: 6 months after treatment; IGHV: immunoglobulin heavy chain variable region; NES: normalized enrichment score; Act.: activation; Prol.: proliferation; CFSE: carboxylfluorescein succinimidyl ester; 12m: 12 months after treatment.

zyme B and IFNγ by flow cytometry upon PMA/Ionomycin stimulation. We observed that the percentages of $CD107a^+$ and granzyme B^+ $CD8^+$ T cells, as well as $IFN\gamma^+$ $CD8^+$ and $CD4^+$ T cells, were not altered by ibrutinib and they were superior than the HD values for the cytotoxic proteins (Figure 3E). Lastly, in order to assess whether treatment with ibrutinib can induce changes in the capacity of T cells to secrete soluble proteins, we stimulated the T cells with beads coated with anti-CD3/CD28 for 3 days and analyzed the cell supernatants from patients BT and after 6 and 12 months of treatment with ibrutinib. We subsequently assessed the concentration of several soluble proteins related to immune response (IL-2, IL-4, IL-6, IL-10, IL17A, IFNγ, TNFα, Fas, FasL, granzyme A, granzyme B, perforin, and granulysin). Our results indicate that after 12 months of ibrutinib treatment, T cells from CLL patients secrete higher levels of IL-2, IL-4, IL-6, IL-10, IL-17A, IFNγ, TNFα, Fas and granzyme B compared to BT whereas the secretion of FasL, granzyme A, perforin and granulysin did not significantly changed, although all showed a tendency to increase (*Online Supplementary Figure S9*). The production of IL-2, IL-4, IFNγ, TNFα, Fas and perforin was comparable, or superior compared to HD T cells, whereas the levels of IL-6, IL-10, IL-17A, FasL, and granzymes, even the observed increased induced by ibrutinib, did not reach HD levels. These results suggest a potentially improved cytotoxic capacity of T cells from patients with CLL after treatment with ibrutinib.

Ibrutinib reduces the concentration of plasma chemokines related to inflammation and migration.

An increase of different inflammatory and regulatory cytokines and chemokines in plasma has been previously reported in CLL patients compared to healthy donors.[29] Due to the crucial role that cytokines and chemokines play in the interactions of CLL cells with the microenvironment, we aimed to measure the plasma concentration of chemokines related to inflammation (CCL2, CCL3, CCL4, CXCL10) and migration/homing to the tumor niche (CXCL13, CCL19, CXCL12) in paired samples obtained at BT and after 6 months of ibrutinib from 18 CLL patients. We observed a decrease of the levels of all the assessed chemokines (Figure 4), indicating that ibrutinib reduced the inflammatory state and homing signals during BTK inhibition treatment.

Chronic lymphocytic leukemia cells show reduced expression of immunosuppression, adhesion, and migration-related proteins and upregulation of CXCR4 expression upon ibrutinib treatment

Next, we characterized longitudinal changes in the surface expression of proteins related to immunosuppression (CD200, BTLA, PD-L1, PD-1), adhesion (CD44, CD62L, CD49d), and migration (CXCR5, CCR7, CXCR4) on CLL cells during 12 months of ibrutinib treatment (Figures 5A-C; *Online Supplementary Figure S10A-C.*). We observed a marked reduction of the levels of expression of CD200 and BTLA (Figure 5A; *Online Supplementary Figure S10A*), while the percentage of $PD\text{-}L1^+$ CLL cells only significantly decreased when we analyzed samples with more than 10% positive cells at baseline (Figure 5A; *Online Supplementary Figure S10A*). Remarkably, PD-1 expression, a marker of B regulatory function also expressed by CLL cells,[30] was strongly reduced after 1 month and maintained after 12 months

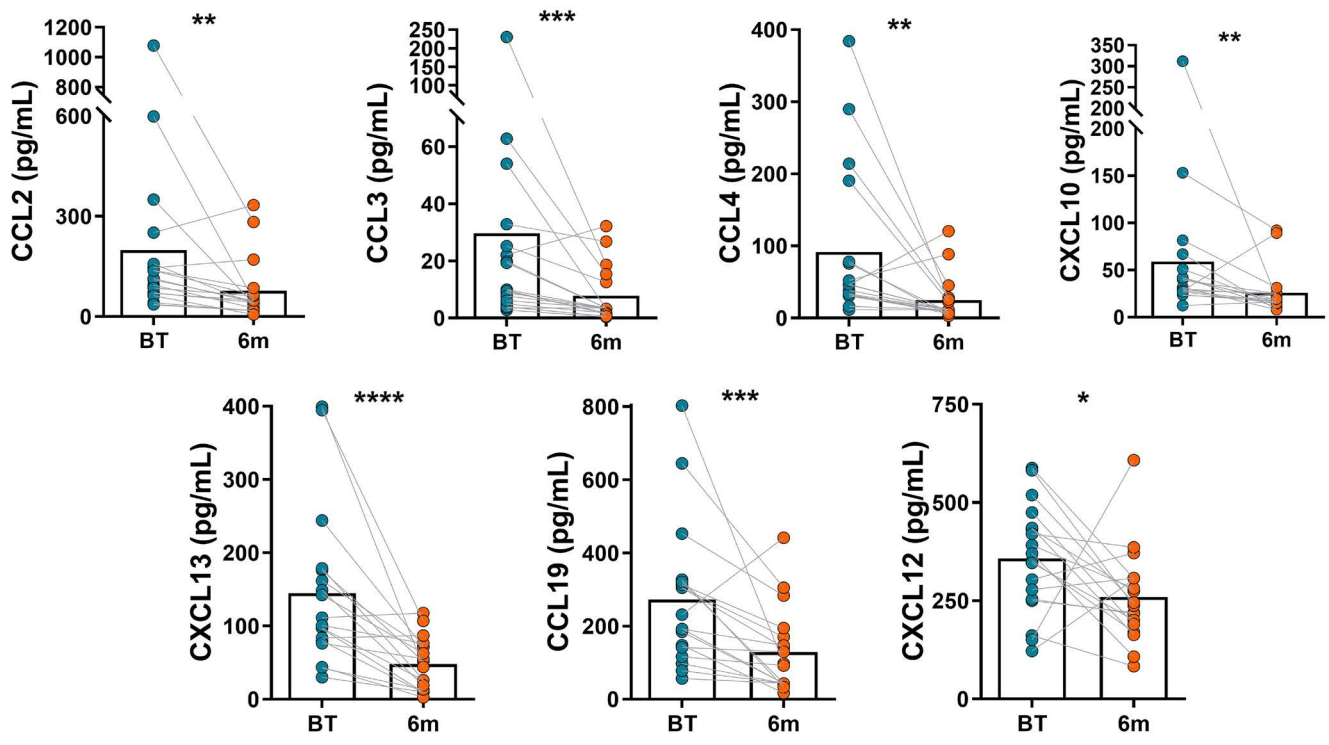

Figure 4. Changes in the concentration of chemokines related to inflammation (CCL2, CCL3, CCL4 and CXCL10) and migration in plasma (CXCL13, CCL19 and CXCL12) (N=19). Wilcoxon matched paired signed rank test was performed to compare statistical differences between before treatment (BT) and 6 months after treatment (6m). Graphs show individual values and mean. *P<0.05; **P<0.01; ***P<0.001; ****P<0.0001.

(Figure 5A; *Online Supplementary Figure S10A*). Regarding adhesion molecules, we observed a decreased expression of CD44 and CD62L, while the percentage of CD49d^{+} CLL cells remained stable (Figure 5B; *Online Supplementary Figure S10B*). Overall, ibrutinib treatment induced a CLL phenotype compatible with reduced capacity to immunomodulate T cells and reside in secondary lymphoid organs. Regarding markers related to chemotaxis, there was a decrease of the expression of CXCR5 and CCR7 (Figure 5C; *Online Supplementary Figure S10C*). Conversely, CXCR4

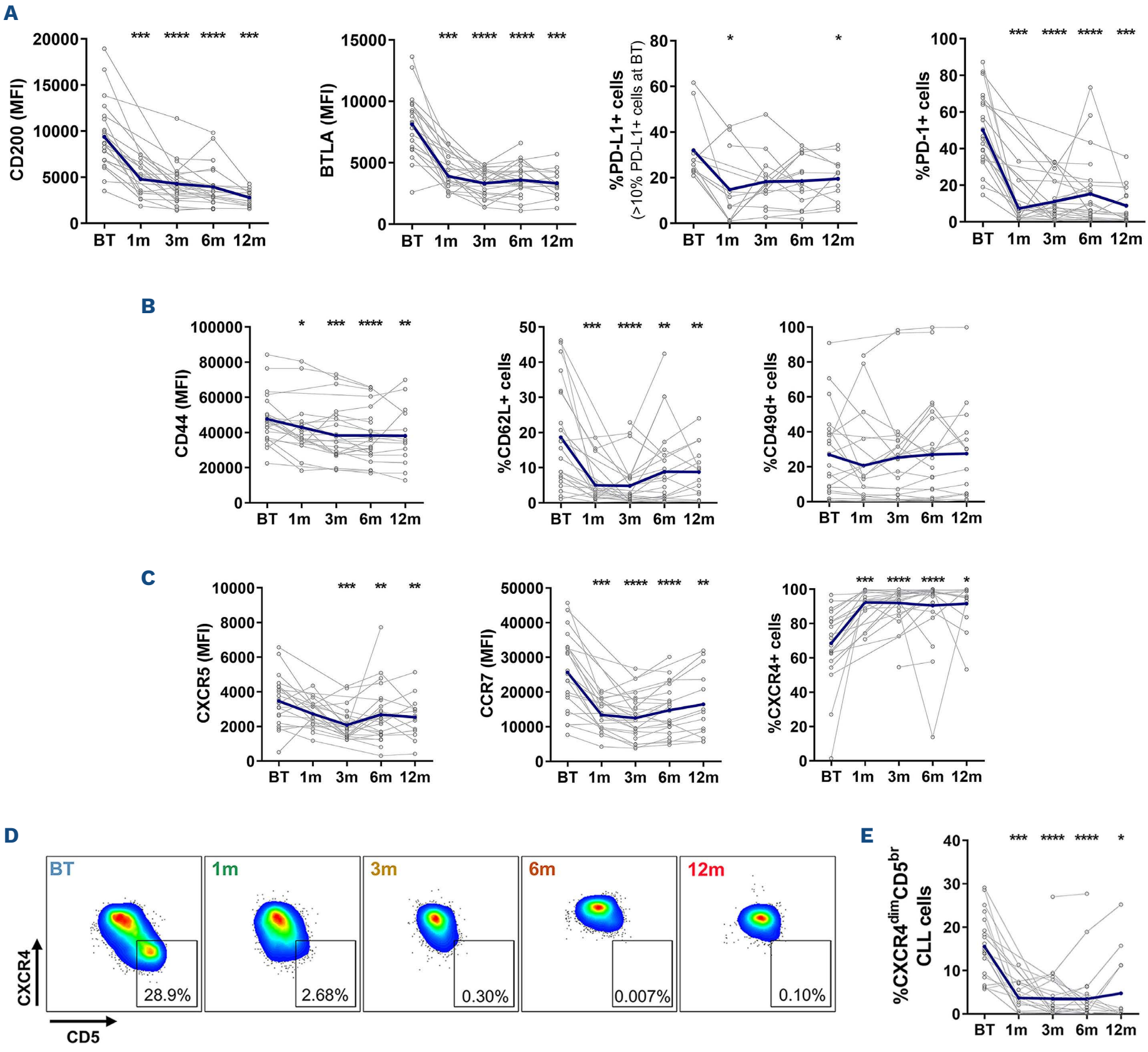

Figure 5. Ibrutinib altered immunosuppression, adhesion, and migration proteins in chronic lymphocytic leukemia cells. (A) Longitudinal analysis of the CD200, BTLA, PD-L1 and PD-1 expressions on CLL cells during ibrutinib treatment. The percentage of PD-L1 expressing chronic lymphocytic leukemia (CLL) cells is only represented for the patients with >10% of expression at before treatment (BT). (B) Longitudinal analysis of the CD44, CD62L and CD49d expressions on CLL cells during ibrutinib treatment. (C) Longitudinal analysis of the CXCR5, CCR7 and CXCR4 expressions on CLL cells during ibrutinib treatment. (D) Representative dot plots of the proliferative population of CLL cells CXCR4^{dim}CD5^{br}. (E) Dynamics of the percentage of CXCR4^{dim}CD5^{br} cells out of CLL cells. Flow cytometry analyses included BT N=21, 1 months after treatment (1m) N=15, 3m N=22, 6m N=24 and 12m N=14 samples. Wilcoxon matched paired signed rank test was performed to compare statistical differences between BT and the subsequent time points. Grey lines represent the dynamics of individual patients, while the blue line represents the mean values across all patients. *P<0.05; **P<0.01; ***P<0.001; ****P<0.0001. MFI: mean fluorescence intensity; Dim: low expression; Br: bright i.e., high expression.

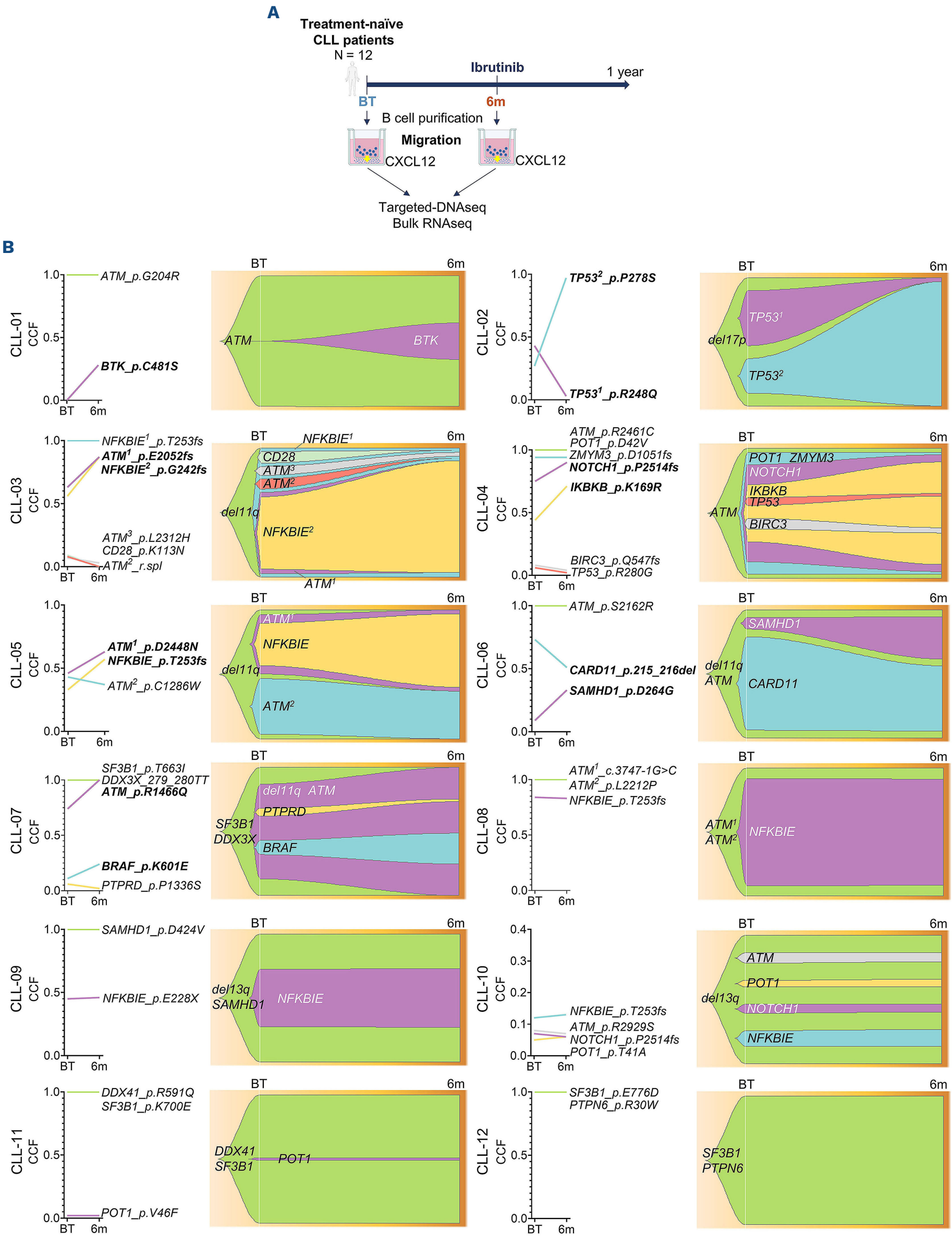

Continued on following page.

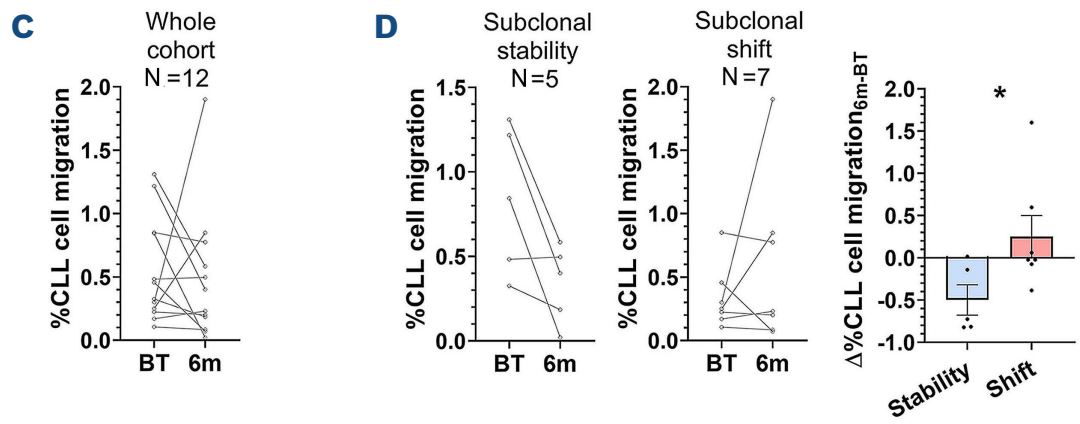

Figure 6. Molecular subclonal changes after 6 months of ibrutinib treatment in chronic lymphocytic leukemia cells with migrative capacity. (A) Migration assays of purified B cells from samples before treatment (BT) and 6 months after ibrutinib treatment (6m) of 12 chronic lymphocytic leukemia (CLL) patients were performed and analyzed by targeted DNA sequencing (targeted-DNAseq) and bulk RNA sequencing (RNAseq). (B) Representation of the changes in cancer cell fraction (CCF) of the subclones detected by targeted-DNAseq between migrated CLL cells from BT and 6m and phylogenetic model inferred represented by Fish plots. Multiple mutations with a CCF <0.1 in the same patient were considered different subclones. (C) Changes in the percentage of specific CLL cell migration before and after ibrutinib treatment towards CXCL12/CXCR4 axis (N=12). (D) Changes of the percentage of specific CLL cell migration of patients exhibiting subclonal stability (N=5) and patients exhibiting subclonal shifts (N=7) and the difference between ibrutinib-treated samples and BT of both groups. Wilcoxon matched paired signed rank test was performed to compare statistical differences between BT and 6m. Grey lines represent the dynamics of individual patients and bars represent mean with standard error of the mean. *P<0.05; **P<0.01; ***P<0.001; ****P<0.0001.

expression was upregulated after just 1 month of treatment, at which point most malignant cells became CXCR4 positive (Figure 5C; *Online Supplementary Figure S10C*). Thus, ibrutinib treatment leads to CXCR4 upregulation but an impaired ability to return to secondary lymphoid organs where cells receive crucial proliferative and survival signaling.[5,31,32] CLL cells with CXCR4^{dim}CD5^{br} phenotype are known to have recently egressed from LN or BM and thus exhibit a proliferative status.[33] Herein we observed that ibrutinib treatment induced an early depletion of these CLL cells in PB, when most of the malignant clone exhibited a quiescent phenotype (Figure 5D, E), probably due to the diminished ability of CLL cells to recirculate between different cellular compartments during BTK inhibition.

Subclonal shifts are associated with retained migrative capacity of chronic lymphocytic leukemia cells upon 6 months of ibrutinib treatment including cells carrying the *BTK* C481S mutation

Treatment with ibrutinib reduces the migrative capacity of CLL cells, which *in vitro* is observed by a diminished proportion of CLL cells migrating towards CCL19, CXCL12 and CXCL13.[34] We hypothesized that this small subset of *ex vivo* migrating cells represent those that are still capable of accessing the nurturing microenvironment and thus may be implicated in the escape from BTK inhibition eventually leading to disease progression. Thus, to characterize this subpopulation of CLL cells, we performed an analysis of the changes observed in the molecular subclonal composition and in the transcriptional program of CLL cells that retained the ability to migrate towards CXCL12 under BTK inhibition. To do so, purified B cells obtained at BT and after 6 months of ibrutinib treatment from 12 patients were allowed to migrate towards CXCL12 in transwells. Transmigrated cells were then collected from the bottom chamber of the transwells for further targeted-DNAseq and bulk RNAseq (Figure 6A).

Targeted-DNAseq revealed that, in seven of 12 patients (CLL-01 to 07), CLL cells with retained migratory capacity after 6 months of ibrutinib displayed a subclonal molecular shift, defined as a differential cancer cell fraction (dCCF) >0.1 (Figure 6B). This change was however non-specific for migrating cells since the same shifts were observed in non-migrating CLL cells (*Online Supplementary Figure S11*). Interestingly, in one patient, we identified a *BTK* C481S mutant subclone. This mutation was detected exclusively in the fraction of cells retaining CXCR4-mediated migratory capacity after 6 months of ibrutinib treatment and represented a CCF of 0.28. This mutated subpopulation was undetectable in the non-migrating fraction or BT samples. Although our NGS analysis was not sensitive enough to detect *BTK* C481S cells in the bulk of CLL cells after 6 months of treatment (limit 1% variant allele frequency [VAF]), considering the percentage of CLL cells able to migrate to CXCL12 after 6 months of ibrutinib in this patient, CLL cells carrying the *BTK* C481S represented only a 0.23% of total circulating CLL cells (patient CLL-01 in Figure 6B; *Online Supplementary Figure S11*). This indicates that the *BTK* C481S mutation after 6 months of treatment is present in only a very small proportion of circulating malignant cells, but most of them maintain their migrative capacity.

We observed heterogeneity in the effect of ibrutinib on inhibiting CLL cells migrative capacity, however, stratification of patients based on molecular changes showed that subclonal shifts in CLL cells associated with higher capacity to retain migration compared to clonal stability including BTK-mutant subclones among others (Figure 6C,

D). This result suggests that specific molecular alterations may overcome BTK inhibition and restore homing capacities.

Chronic lymphocytic leukemia cells that maintain migratory capacity during ibrutinib treatment upregulate survival and proliferation pathways

We and others have observed how treatment with ibrutinib impairs but does not completely block migrative capacity of CLL cells. Also, in some cases, subclonal populations of mutated CLL cells have different migrative capacities, as earlier described. In addition, we hypothesized that the subpopulation of CLL cells that retains this capacity during BTK inhibition has a differential gene expression, which could be interrogated to identify potential therapeutic targets. To elucidate that, we analyzed the gene expression profile of those cells that, even under treatment with ibrutinib, are still able to migrate to CXCL12 compared to migrating cells before treatment. This was performed by allowing purified B cells obtained at BT and after 6 months of ibrutinib treatment from 12 patients to migrate towards CXCL12 in transwells. Transmigrated cells were then collected from the bottom chamber of the transwells and RNAseq was performed.

Differential expression analysis revealed only 15 significant DEG (at 6 months compared to BT), which did not show a clear clustering pattern according to ibrutinib treatment in the unsupervised analysis (Figure 7A; *Online Supplementary Table S8)*. However, further GSEA, revealed upregulation of pathways related to activation, survival, and proliferation, reflecting the recent entry in proliferative centers of CLL cells with retained CXCR4-migratory capacity under BTK inhibition (Figure 7B; *Online Supplementary Table S8*). Notably, mTORC1 signaling and MYC signaling pathways were among the significantly enriched pathways (Figure 7C), both being related to high-risk CLL and adaptation to ibrutinib treatment.[35-38] Altogether, these results show that CLL cells that are still able to migrate to CXCL12 *in vitro* after ibrutinib treatment exhibit a transcriptome associated with increased aggressiveness.

The characterization of adaptive mechanisms to short-term BTK inhibition could facilitate the identification of potential new targets. We investigated the potential prognosis value of the DEG observed in the cells with retained migratory capacity under ibrutinib using public data from the CLL-map portal.[39] By matching batch-corrected RNAseq expression from 603 CLL patients and overall survival (OS) from 1,009 patients, we studied a cohort of 566 CLL patients (*Online Supplementary Table S9*). Among the downregulated genes,

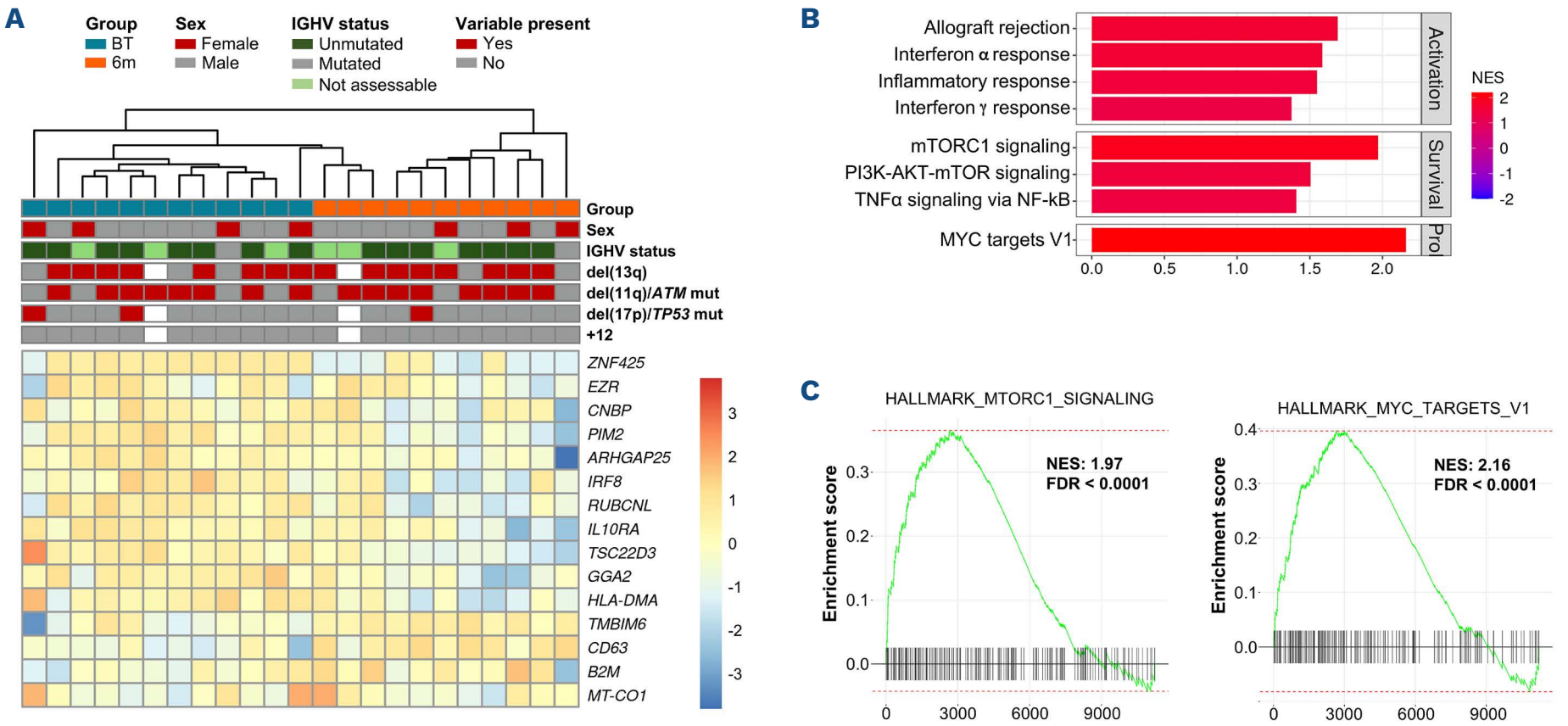

Figure 7. Transcriptomic analysis of chronic lymphocytic leukemia cells with retained CXCR4-mediated migration. (A) Clustered heatmap of the 15 differential expressed genes (DEG) (false discovery rate [FDR] < 0.05) in chronic lymphocytic leukemia (CLL) cells with conserved CXCR4-migratory capacity under Bruton tyrosine kinase (BTK) inhibition compared to migrated cells before treatment (BT). One of the samples from the 6 months after treatment (6m) group was excluded for low quality RNA. (B) Summary of the significant enriched processes (FDR <0.05) from the gene set enrichment analysis (GSEA) against Hallmarks from MSigDB of RNA sequencing (RNAseq) of CLL cells from BT and 6m CXCL12-migrated cells. (C) GSEA plots of mTORC1 signaling and MYC Targets V1 from RNAseq of migrating cells at 6m compared to BT. (D) Changes in *TMBIM6* expression in CXCL12-migrated cells. IGHV: immunoglobulin heavy chain variable region; NES: normalized enrichment score; Prol.: proliferation.

we observed that low expression of *IL10RA* and *ARHGAP2* robustly associated with poor overall survival (OS) and failure-free survival (FFS) (*Online Supplementary Figure S12*). Among the upregulated genes, high expression of *TMBIM6* and *CD63* strongly correlated with poor OS and FFS in CLL suggesting that this high expression leads to a more aggressive disease (*Online Supplementary Figure S12*).

TMBIM6 (transmembrane Bax inhibitor motif containing 6) is a negative regulator of apoptosis, and its interaction with the mTORC2 complex leading to AKT signaling activation has recently been reported.[40,41] We further explored the prognostic value of the expression of *TMBIM6* in CLL as a significantly upregulated gene with the highest association with worse prognosis (Figure 7D; *Online Supplementary Figures S12* and *S13A, B*). High expression of TMBIM6 was independently associated with poor prognosis, regardless of age, sex, IGHV mutational status, del(11q), del(17p), *TP53* mutations or amp(12) (*Online Supplementary Figures S14A, B* and *S15A*). The expression of *TMBIM6*, located on chromosome 12, was higher in patients with amp(12). Interestingly, those patients with high *TMBIM6* expression and amp(12) demonstrated a significantly inferior OS (*Online Supplementary Figure S15B, C*). Kim *et al*. previously identified BIA as an antagonist of TMBIM6. BIA refers to the synthesized molecule (E)-1-(2-aminophenyl)-3-(3-nitrophenyl)prop-2-en-1-one, a chalcone derivative that prevents TMBIM6 binding to mTORC2, decreases mTORC2 activity and also regulates TMBIM6-leaky Ca^{2+}.[41] BIA has demonstrated inhibitory effects on the proliferation of various neoplastic cell lines.[41] Thus, we investigated TMBIM6 as a potential target for CLL and evaluated the effect of BIA on CLL cells. BIA induced dose-dependent apoptosis in a co-culture system composed by PBMC from CLL patients with UE6E7T-2 BMSC, CD40L and ODN CpG that we previously reported as mimicking the LN or BM microenvironment (Figure 8A).[19] BIA concentrations ranged from 1 μM to 10 μM, based on their negligible effect on TMBIM6 KO cells as previously reported by Kim *et al*.. Interestingly, the effect of BIA on T cells in suspension cultures was only observed at higher concentrations, indicating less sensitivity of T cells to TMBIM6 inhibition (Figure 8B; *Online Supplementary Figure S16A-C*). To evaluate the potential synergistic effect of BIA in combination with ibrutinib, we used the co-culture setup previously mentioned. We observed that the combination of BIA and ibrutinib was able to induce apoptosis. Additionally, at higher concentrations of ibrutinib, the addition of BIA produced a synergistic effect (Figure 8C; *Online Supplementary Figure S16D*). These results suggest that BIA and ibrutinib target distinct pathways that inhibit CLL survival. Collectively, our results revealed TMBIM6 as a potential therapeutic target in CLL, either alone or in combination with a BTK inhibitor.

Discussion

Unravelling the complex interplay between CLL cells and the tumor immune microenvironment is crucial for understanding disease progression and the emergence of treatment resistances. Here, we aimed to decipher the modulations in the CLL microenvironment induced after short-term ibrutinib treatment to identify potential adaptation mechanisms that may lead to disease progression and, eventually, be targeted using novel therapeutic combinations.

The analysis of T cells revealed a decreased expression of exhaustion markers, the frequency of Th subpopulations and Tregs, as well as downregulation of genes related to T-cell activation, differentiation, metabolism, and proliferation. While similar immunophenotypic changes have been observed in previous studies,[11,12,42] limited research has reported transcriptomic changes in T cells. Rendeiro *et al*.[43] reported a downregulation of several activation pathways in T cells of patients receiving ibrutinib in the relapse/refractory setting through single-cell RNAseq after 120 days, which aligns with our findings after 6 months of upfront treatment.[43] At a functional level, T-cell proliferation slightly improved upon ibrutinib treatment whereas cytokine production was retained after 12 months of therapy similarly to previous reports. However, different *ex vivo* approaches for stimulating T cells, including days of proliferation, can account for the modest effects by ibrutinib herein described.[8,12,42,44] The reduction of the CLL inflammatory burden and the off-target effects of ibrutinib may contribute to the downregulation of several pathways in T cells. Supporting this, we observed a reduction of pro-inflammatory and migratory chemokines in plasma. Based on our and previous observations, treatment with ibrutinib can potentially improve T-cell function, which could be related to decreased risk of secondary malignancies, as observed in CLL12 trial, although patients under BTKi still remain at high risk.[45] Also, however, immunosuppression caused by inhibition of BTK in B cells is related to poor serological response to vaccines and higher risk of infections.[46]

The immunophenotyping of CLL cells, consistent with previous studies, showed a downregulation of surface markers related to immunosuppression, adhesion, and migration after 12 months of ibrutinib treatment.[12,31] Notably, the regulatory marker PD-1 showed significant downregulation.[47] Additionally, ibrutinib induced a significant upregulation of CXCR4 expression, as the proliferative fraction of $CXCR4^{dim}CD5^{br}$ was depleted. This overexpressed CXCR4 has been previously observed and been related to diminished phosphorylation upon CXCL12 stimulation.[48] Overall, these features indicate that after 12 months of treatment with ibrutinib, the interaction of cytotoxic T cells and malignant CLL cells generate the potential to be targeted by currently developing T-cell engager immunotherapies. Not only do T cells have a less immunosuppressed phenotype after 12 months of treatment with ibrutinib, but malignant cells diminish their numbers and immunosuppressive features, feeding the positive feedback loop towards potentially increased cytotoxicity of T cells. Moreover, the effec-

tor-to-target ratio increases as the number of malignant cells decreases. This could then be leveraged to design timely optimized combination therapies that not only engage cytotoxic T cells but previously debulk malignant cells and improve immune fitness. In this regard, Mhibik *et al.*[49] have observed increased sensitivity of CLL cells from ibrutinib-treated patients to bispecific antibodies *ex vivo* compared to untreated patients. Also, exposure to ibrutinib has been shown to enhance the performance of chimeric antigen receptor T cells.[44]

In this scenario of ongoing BTK inhibition, certain CLL cells are still able to access a nurturing microenvironment. This likely sustains a small but persistent subpopulation with continuous survival and proliferative signaling, potentially leading to clinical progression. This hypothesis is supported by the fact that continuous treatment with BTKi rarely achieves undetectable minimal residual disease and patients eventually relapse.[50,51] Combinations, such as BTK plus Bcl-2 inhibitors, are pursued to achieve higher rates of CR.[52] For this reason, and under the hypothesis that subclones with

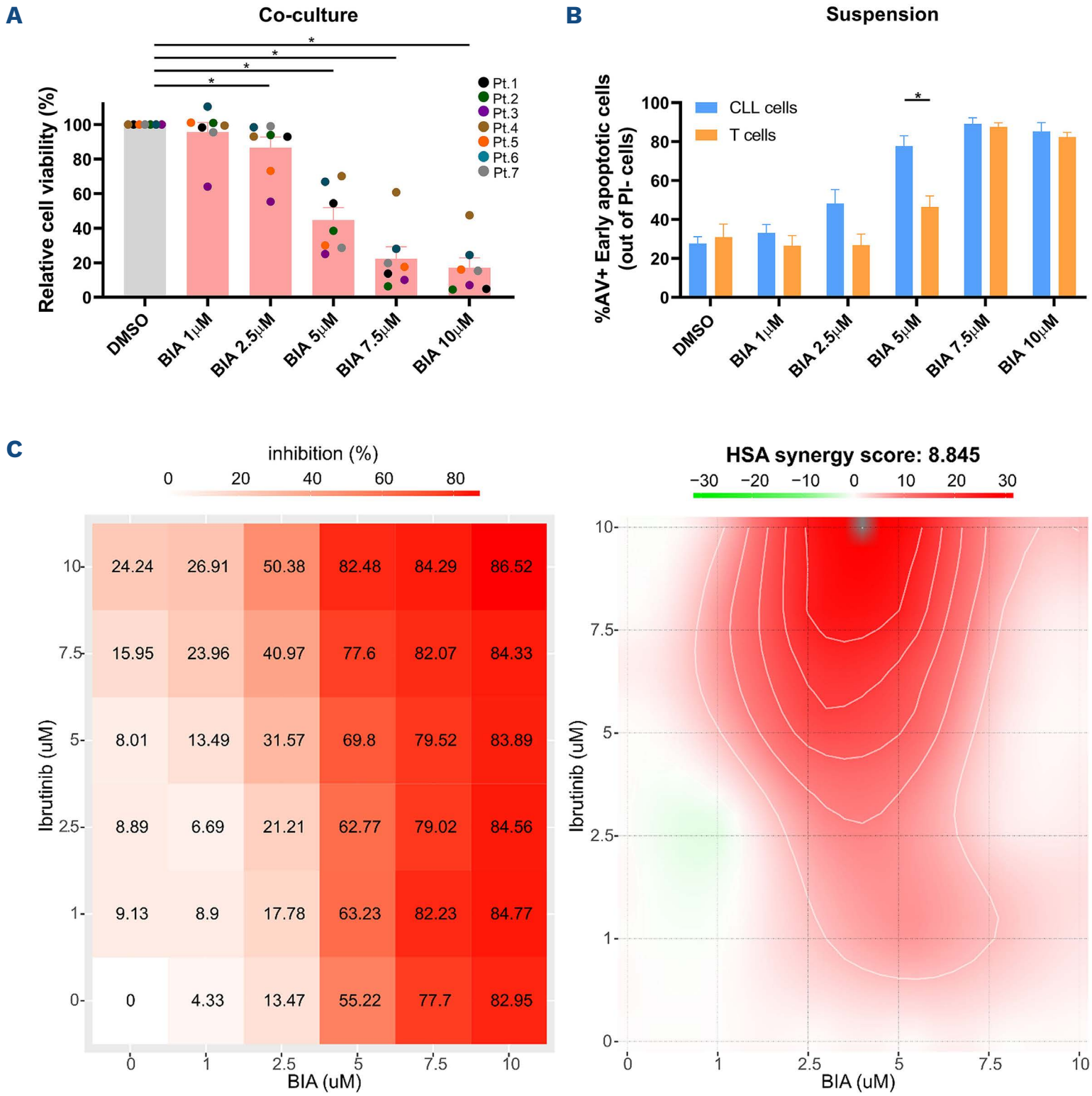

Figure 8. TMBIM6 as a novel target in chronic lymphocytic leukemia. (A) Relative cell viability of peripheral blood mononuclear cells (PBMC) from chronic lymphocytic leukemia (CLL) patients in a co-culture with UE6E7T-2 plus CD40L and CpG ODN upon 24 hours of BIA treatment. Relative cell viability was assessed by normalizing the percentage of annexin V-negative/propidium iodide-negative (AV^-/PI^-) cells. (B) Early apoptotic (AV^+) CLL cells and T cells out of PI^- cells upon 48 hours of BIA treatment in suspension culture. (C) Matrix of relative inhibition of PBMC from CLL patients at different concentrations of BIA combined with ibrutinib and HSA synergy score plots. Wilcoxon matched paired signed rank test was performed to compare statistical differences between concentrations. Graphs show individual values, mean and +/- standard error of the mean. *P<0.05; **P<0.01; ***P<0.001; ****P<0.0001. CpG ODN: CpG oligodeoxynucleotide; Pt.: patient; DMSO: dimethyl sulfoxide; HSA: highest single agent.

retained migrative capacity may be responsible for eventual progression under ibrutinib treatment, we explored the characteristics of these cells to identify novel potential therapeutic targets that could help eradicate CLL cells in a fixed-duration treatment regimen. For this, we physically separated CLL cells with retained migrative capacity under BTK inhibition towards CXCL12 using transwells. We did not observe clinically significant molecular clonal shifts in these migrating CLL cells, however, subclonal shifts associated with retaining of CXCR4-mediated migration upon ibrutinib. Remarkably, in one patient, we detected a subclone carrying the *BTK* C481S resistance mutation at a CCF of 0.28, but only when analyzing CXCL12-responsive CLL cells. This finding shows that these cells lack BCR inhibition, allowing them to access a nurturing microenvironment and potentially drive disease progression.

Transcriptomic analysis of CLL cells with retained migration under BTK inhibition revealed few significant changes, but it showed a clear upregulation of survival and proliferation pathways including mTORC1 and MYC signaling. Increased MYC activity has been recently associated with a LN-phenotype when compared with PB-CLL cells and is also related to high-risk CLL and adaptation to ibrutinib,[35-38,53] highlighting the potential of the analysis to define novel therapeutic targets that are able to eradicate this subset of migrating cells. With this approach, we foresee the design of newer combinations with potential to eradicate minimal residual disease. Therefore, although the overall access to nurturing microenvironment is impaired by BTK inhibition, the subset of malignant cells that are still able to access this microenvironment show transcriptomic characteristics indicative of increased aggressiveness, which could potentially be related to eventual clinical progression.

As a proof of concept, we analyzed *TMBIM6*, one of the most differentially expressed genes in CLL cells retaining migrative capacity after 6 months of ibrutinib treatment. *TMBIM6* encodes for a protein described as a negative regulator of apoptosis and a positive a regulator of the mTOR-AKT axis.[40,41,54] Interestingly, Kim *et al*. identified BIA, a TMBIM6 antagonist that inhibits the interaction between TMBIM6 and mTORC2, ultimately blocking AKT activation. BIA has demonstrated inhibition of tumor growth in *in vitro* and *in vivo*,[41] providing us the opportunity to try the BTK and TMBIM6 inhibition combination which demonstrated a synergistic effect in inducing apoptosis, suggesting that BIA could potentially overcome an adaptive mechanism of CLL cells to ibrutinib treatment. Additional experiments specifically targeting cells adapted to BTK inhibition may elucidate the impact of TMBIM6 inhibition in the eradication of CLL cells. Finally, *TMBIM6* high expression has been associated with poor survival in solid tumors.[41] Our study also demonstrated that *TMBIM6* high expression is associated with poor prognosis in CLL, independent of age, sex, *IGHV* mutational status, del(11q), del(17p), amp(12) and *TP53* mutations. Further pre-clinical investigations are warranted to validate these findings, including the feasibility of targeting TMBIM6 and explore the translational potential of these therapeutic strategies in CLL management.

This study presents some limitations, mainly regarding the small number of patients together with the limited number of cells available to perform the multiple experiments. This limitation also impedes us to stratify patients based on clinical parameters such as sex, *IGHV* status or molecular alterations. Nevertheless, this comprehensive multi-omics study sheds light on the intricate immunomodulatory effects of ibrutinib in CLL patients. The observed changes in immune cell dynamics, T-cell function, and the identification of adaptive mechanisms in malignant cells highlight the potential for targeted therapeutic interventions, such as the combination of BTK and TMBIM6 inhibition, with the aim of eradicating minimal residual disease and improving patient outcomes.

Disclosures

AC has received honoraria from Janssen, AstraZeneca, BeiGene and AbbVie. CF has received from Janssen, Roche, Gilead, Takeda, and AbbVie. MJT has received honoraria from Janssen, BMS, Gilead, AbbVie, Roche, Novartis, Incyte, Amgen, GSK, AstraZeneca, Lilly and Takeda. FB has received honoraria and research funding from BMS, Kite, MSK, Roche, Celgene, Karyopharm, Takeda, AstraZeneca, Novartis, AbbVie, Janssen, Gilead, TG Therapeutics, Allogene, Advantage, Mundipharma, Lilly and BeiGene. PA has received honoraria and research funding from Janssen, Roche, BMS, AbbVie, AstraZeneca, BeiGene, Gilead, Genmab, Regeneron and Incyte. MC has received research funding and honoraria from Janssen, Karyopharm, Genentech, Takeda and AstraZeneca. All remaining authors have no conflicts of interest to disclose.

Contributions

Concept and design were undertaken by DM-G, MC, PA, FB and MM. Samples were provided by AC, PA, FB, CF, MA, MJT and RA. Blood sample processing was performed by DM-G, CP, CH, and GP. Laboratory experiments were conducted by DM-G, LP, GL, CH, OC and BS. Data analysis was conducted by DM-G, LP, VN, GL, CH, BM-M, PMM-T and AE-C. Results were interpreted and discussed by DM-G, LP, GL, MC, PA, FB, MM, OC, BS, CP, CH, and GP. The figures were made by DM-G in collaboration with LP, VN, BM-M and DM-G.MC and FB wrote the manuscript, and it was reviewed and approved by all the contributing authors.

Acknowledgments

The authors thank the patients for their blood donations. The authors also express gratitude to the State Agency for Research (Agencia Estatal de Investigación) for the financial support as a Center of Excellence Severo Ochoa (CEX2020-001024-S/AEI/10.13039/501100011033), the Cellex Foundation for providing research facilities and equipment and the CERCA Programme from the Generalitat de Catalunya for their

support on this research. We are deeply grateful to Alberto López-García for insightful discussions. His contributions and dedication continue to inspire us.

Funding

This work was supported by research funding from the Instituto de Salud Carlos III, Fondo de Investigaciones Sanitarias (PI21/01190, to MC) (PI20/01274 and PI24/00529 to FB), (PI22/01204 PA and Fundació la Marató de TV3 [201905-30-31] to FB). All Spanish funding was co-sponsored by the European Union FEDER program "Una manera de hacer Europa". DM-G holds a contract from Agència de Gestió d'Ajuts Universitaris i de Recerca (AGAUR) (2022FI_B 00092).

Data-sharing statement

Transcriptomic data is available in GEO under the accession number GSE254718. The authors will also provide the original data from targeted-DNA sequencing upon request.

References

1. O'Brien S, Furman RR, Coutre S, et al. Single-agent ibrutinib in treatment-naïve and relapsed/refractory chronic lymphocytic leukemia: a 5-year experience. Blood. 2018;131(17):1910-1919.
2. Burger JA, Barr PM, Robak T, et al. Long-term efficacy and safety of first-line ibrutinib treatment for patients with CLL/SLL: 5 years of follow-up from the phase 3 RESONATE-2 study. Leukemia. 2020;34(3):787-798.
3. Herman SEM, Gordon AL, Hertlein E, et al. Bruton tyrosine kinase represents a promising therapeutic target for treatment of chronic lymphocytic leukemia and is effectively targeted by PCI-32765. Blood. 2011;117(23):6287-6296.
4. Ponader S, Chen S-S, Buggy JJ, et al. The Bruton tyrosine kinase inhibitor PCI-32765 thwarts chronic lymphocytic leukemia cell survival and tissue homing in vitro and in vivo. Blood. 2012;119(5):1182-1189.
5. de Rooij MFM, Kuil A, Geest CR, et al. The clinically active BTK inhibitor PCI-32765 targets B-cell receptor–and chemokine-controlled adhesion and migration in chronic lymphocytic leukemia. Blood. 2012;119(11):2590-2594.
6. Advani RH, Buggy JJ, Sharman JP, et al. Bruton tyrosine kinase inhibitor ibrutinib (PCI-32765) has significant activity in patients with relapsed/refractory B-cell malignancies. J Clin Oncol. 2013;31(1):88-94.
7. Ramsay AG, Johnson AJ, Lee AM, et al. Chronic lymphocytic leukemia T cells show impaired immunological synapse formation that can be reversed with an immunomodulating drug. J Clin Invest. 2008;118(7):2427-2437.
8. Riches JC, Davies JK, McClanahan F, et al. T cells from CLL patients exhibit features of T-cell exhaustion but retain capacity for cytokine production. Blood. 2013;121(9):1612-1621.
9. Jiménez I, Tazón-Vega B, Abrisqueta P, et al. Immunological and genetic kinetics from diagnosis to clinical progression in chronic lymphocytic leukemia. Biomark Res. 2021;9(1):37.
10. Dubovsky JA, Beckwith KA, Natarajan G, et al. Ibrutinib is an irreversible molecular inhibitor of ITK driving a Th1-selective pressure in T lymphocytes. Blood. 2013;122(15):2539-2549.
11. Niemann CU, Herman SEM, Maric I, et al. Disruption of in vivo chronic lymphocytic leukemia tumor–microenvironment interactions by ibrutinib–findings from an investigator-initiated phase II study. Clin Cancer Res. 2016;22(7):1572-1582.
12. Long M, Beckwith K, Do P, et al. Ibrutinib treatment improves T cell number and function in CLL patients. J Clin Invest. 2017;127(8):3052-3064.
13. Wiestner A. The role of B-cell receptor inhibitors in the treatment of patients with chronic lymphocytic leukemia. Haematologica. 2015;100(12):1495-1507.
14. Herman SEM, Montraveta A, Niemann CU, et al. The Bruton tyrosine kinase (BTK) inhibitor acalabrutinib demonstrates potent on-target effects and efficacy in two mouse models of chronic lymphocytic leukemia. Clin Cancer Res. 2017;23(11):2831-2841.
15. Puzzolo MC, Del Giudice I, Peragine N, et al. TH2/TH1 shift under ibrutinib treatment in chronic lymphocytic leukemia. Front Oncol. 2021;11:637186.
16. Woyach JA, Furman RR, Liu T-M, et al. Resistance mechanisms for the Bruton's tyrosine kinase inhibitor ibrutinib. N Engl J Med. 2014;370(24):2286-2294.
17. Abrisqueta P, González-Barca E, Ferrà C, et al. Ibrutinib followed by ofatumumab consolidation in previously untreated patients with chronic lymphocytic leukemia (CLL): GELLC-7 trial from the Spanish group of CLL (GELLC). EClinicalMedicine. 2024;73:102642.
18. Picelli S, Faridani OR, Björklund ÅK, Winberg G, Sagasser S, Sandberg R. Full-length RNA-seq from single cells using Smart-seq2. Nat Protoc. 2014;9(1):171-181.
19. Purroy N, Abrisqueta P, Carabia J, et al. Co-culture of primary CLL cells with bone marrow mesenchymal cells, CD40 ligand and CpG ODN promotes proliferation of chemoresistant CLL cells phenotypically comparable to those proliferating in vivo. Oncotarget. 2015;6(10):7632-7643.
20. Zheng S, Wang W, Aldahdooh J, et al. SynergyFinder plus: toward better interpretation and annotation of drug combination screening datasets. Genomics Proteomics Bioinformatics. 2022;20(3):587-596.
21. Jain P, Javdan M, Feger FK, et al. Th17 and non-Th17 interleukin-17-expressing cells in chronic lymphocytic leukemia: delineation, distribution, and clinical relevance. Haematologica. 2012;97(4):599-607.
22. Cha Z, Zang Y, Guo H, et al. Association of peripheral CD4+ CXCR5+ T cells with chronic lymphocytic leukemia. Tumor Biol. 2013;34(6):3579-3585.
23. Palma M, Gentilcore G, Heimersson K, et al. T cells in chronic lymphocytic leukemia display dysregulated expression of immune checkpoints and activation markers. Haematologica. 2017;102(3):562-572.
24. Catakovic K, Gassner FJ, Ratswohl C, et al. TIGIT expressing CD4+ T cells represent a tumor-supportive T cell subset in chronic lymphocytic leukemia. Oncoimmunology. 2017;7(1):e1371399.
25. D'Arena G, Laurenti L, Minervini MM, et al. Regulatory T-cell number is increased in chronic lymphocytic leukemia patients and correlates with progressive disease. Leuk Res. 2011;35(3):363-368.
26. Pascutti MF, Jak M, Tromp JM, et al. IL-21 and CD40L signals from autologous T cells can induce antigen-independent proliferation of CLL cells. Blood. 2013;122(17):3010-3019.
27. Supek F, Bošnjak M, Škunca N, Šmuc T. REVIGO summarizes

and visualizes long lists of gene ontology terms. PLoS One. 2011;6(7):e21800.
28. Steen CB, Liu CL, Alizadeh AA, Newman AM. Profiling cell type abundance and expression in bulk tissues with CIBERSORTx. Methods Mol Biol. 2020;2117:135-157.
29. Yan X-J, Dozmorov I, Li W, et al. Identification of outcome-correlated cytokine clusters in chronic lymphocytic leukemia. Blood. 2011;118(19):5201-5210.
30. Kondo K, Shaim H, Thompson PA, et al. Ibrutinib modulates the immunosuppressive CLL microenvironment through STAT3-mediated suppression of regulatory B-cell function and inhibition of the PD-1/PD-L1 pathway. Leukemia. 2018;32(4):960-970.
31. Herman SEM, Mustafa RZ, Jones J, Wong DH, Farooqui M, Wiestner A. Treatment with Ibrutinib inhibits BTK-and VLA-4-dependent adhesion of chronic lymphocytic leukemia cells in vivo. Clin Cancer Res. 2015;21(20):4642-4651.
32. Chen S-S, Chang BY, Chang S, et al. BTK inhibition results in impaired CXCR4 chemokine receptor surface expression, signaling and function in chronic lymphocytic leukemia. Leukemia. 2016;30(4):833-843.
33. Calissano C, Damle RN, Marsilio S, et al. Intraclonal complexity in chronic lymphocytic leukemia: fractions enriched in recently born/divided and older/quiescent cells. Mol Med. 2011;17(11-12):1374-1382.
34. Rey-Barroso J, Munaretto A, Rouquié N, et al. Lymphocyte migration and retention properties affected by ibrutinib in chronic lymphocytic leukemia. Haematologica. 2024;109(3):809-823.
35. Cosimo E, Tarafdar A, Moles MW, et al. AKT/mTORC2 inhibition activates FOXO1 function in CLL cells reducing B-cell receptor-mediated survival. Clin Cancer Res. 2019;25(5):1574-1587.
36. Lu J, Cannizzaro E, Meier-Abt F, et al. Multi-omics reveals clinically relevant proliferative drive associated with mTOR-MYC-OXPHOS activity in chronic lymphocytic leukemia. Nat Cancer. 2021;2(8):853-864.
37. Kohlhaas V, Blakemore SJ, Al-Maarri M, et al. Active Akt signaling triggers CLL toward Richter transformation via overactivation of Notch1. Blood. 2021;137(5):646-660.
38. Seda V, Vojackova E, Ondrisova L, et al. FoxO1-GAB1 axis regulates homing capacity and tonic AKT activity in chronic lymphocytic leukemia. Blood. 2021;138(9):758-772.
39. Knisbacher BA, Lin Z, Hahn CK, et al. Molecular map of chronic lymphocytic leukemia and its impact on outcome. Nat Genet. 2022;54(11):1664-1674.
40. Zhang M, Li X, Zhang Y, Zhou K. Bax inhibitor-1 mediates apoptosis-resistance in human nasopharyngeal carcinoma cells. Mol Cell Biochem. 2010;333(1-2):1-7.
41. Kim H-K, Bhattarai KR, Junjappa RP, et al. TMBIM6/BI-1 contributes to cancer progression through assembly with mTORC2 and AKT activation. Nat Commun. 2020;11(1):4012.
42. Solman IG, Blum LK, Hoh HY, et al. Ibrutinib restores immune cell numbers and function in first-line and relapsed/refractory chronic lymphocytic leukemia. Leuk Res. 2020;97:106432.
43. Rendeiro AF, Krausgruber T, Fortelny N, et al. Chromatin mapping and single-cell immune profiling define the temporal dynamics of ibrutinib response in CLL. Nat Commun. 2020;11(1):577.
44. Fraietta JA, Beckwith KA, Patel PR, et al. Ibrutinib enhances chimeric antigen receptor T-cell engraftment and efficacy in leukemia. Blood. 2016;127(9):1117-1127.
45. Langerbeins P, Robrecht S, Nieper P, et al. Ibrutinib in early-stage chronic lymphocytic leukemia: the randomized, placebo-controlled, double-blind, phase III CLL12 trial. J Clin Oncol. 2025;43(4):392-402.
46. Jiménez M, Fernández-Naval C, Navarro V, et al. Kinetics of cellular and humoral immunogenicity and effectiveness of SARS-CoV-2 booster vaccination in hematologic neoplasms. Am J Hematol. 2023;98(8):1204-1213.
47. Xiao X, Lao X-M, Chen M-M, et al. PD-1hi identifies a novel regulatory B-cell population in human hepatoma that promotes disease progression. Cancer Discov. 2016;6(5):546-559.
48. Chen S, Chiorazzi N. Functional consequences of inhibition of Bruton's tyrosine kinase by ibrutinib in chronic lymphocytic leukemia. Hematol Oncol. 2023;41(Suppl 1):119-128.
49. Mhibik M, Gaglione EM, Eik D, et al. Cytotoxicity of the CD3× CD20 bispecific antibody epcoritamab in CLL is increased by concurrent BTK or BCL-2 targeting. Blood Adv. 2023;7(15):4089-4101.
50. Ailawadhi S, Parrondo RD, Paulus A, et al. Time-limited maintenance with ibrutinib after first-fine therapy and the incremental impact on minimal residual disease (MRD) for patients with chronic lymphocytic leukemia (CLL). Blood. 2022;140(Suppl 1):9904-9905.
51. Itsara A, Sun C, Bryer E, et al. Long-term outcomes in chronic lymphocytic leukemia treated with ibrutinib: 10-year follow-up of a phase 2 study. Blood. 2023;142(Suppl 1):201.
52. Jain N, Keating M, Thompson P, et al. Ibrutinib and venetoclax for first-line treatment of CLL. N Engl J Med. 2019;380(22):2095-2103.
53. Sun C, Chen Y-C, Martinez Zurita A, et al. The immune microenvironment shapes transcriptional and genetic heterogeneity in chronic lymphocytic leukemia. Blood Adv. 2023;7(1):145-158.
54. Hsu C-F, Sui C-L, Wu W-C, et al. Klf10 induces cell apoptosis through modulation of BI-1 expression and Ca2+ homeostasis in estrogen-responding adenocarcinoma cells. Int J Biochem Cell Biol. 2011;43(4):666-673.